Exploring Dynamical Status and High Energy Phenomena of Merging Galaxy Clusters with Multi-band Observations

Motokazu Takizawa

(Yamagata University)

Abell 2319: Sugawara,Takizawa, & Nakazawa (2009)

ZwCl0823.2+0425 Field: Watanabe, Takizawa et al. (2011)

Imaging simulations of SZ Effect for ALMA: Yamada et al. (2012, in press)

High Energy Phenomena of Clusters of Galaxies

Non-thermal radio emission from merging clusters of galaxies

synchrotron radio

$\gamma \sim 10^4$ electrons + 0.1-10μG B

Hard X-ray will be emitted through Inverse compton with CMB

Abell 2319 with Radio Halo
Rosat X-ray image (colors)
Radio image (contours)
Feretti et al. 1997

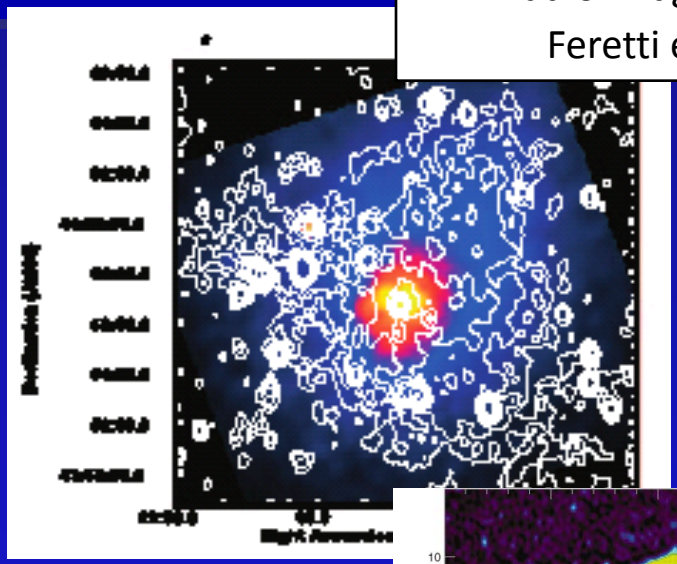

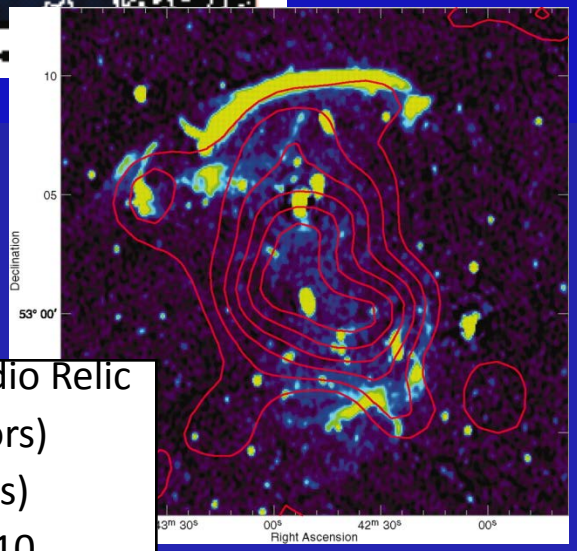

CIZA J2242.8+5301 with Radio Relic
Rosat X-ray image (colors)
Radio image (contours)
Van Weeren et al. 2010

Particle acceleration and Gas Motion

- Particle acceleration processes are likely related with magnetized plasma motion.

  shocks or magetic turbulence or ???

- Information about "gas motion" , "high energy particles" , and "magnetic field" are crucial.
- "X-ray spectroscopy with high energy resolution", "Hard X-ray observation", and radio observations are necessary.

Before Suzaku

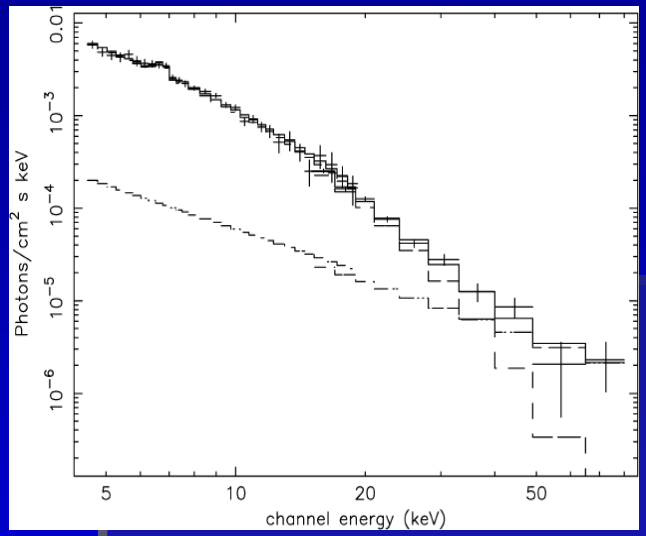

Detection of Non-thermal hard X-ray from Coma by B-SAX?? (Fusco-Femiano et al. 1999, 2005etc)

Possible detection of gas bulk motion (～1500km/s) by ASCA and Chandra,,,,,,,,
(Dupke et al. 2001 for Centaurus cluster etc）

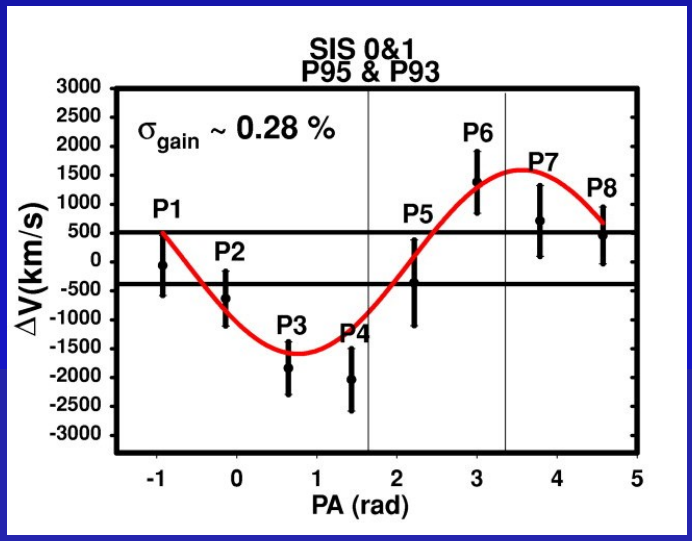

However, later Suzaku results are negative for the both. (Wik et al 2009, Ohta et al. 2006 etc）。

Abell 2319

- Nearby (z=0.0557) well-known merging cluster with a giant radio halo
- Two subgroups are found in radial velocity distribution of the member galaxies

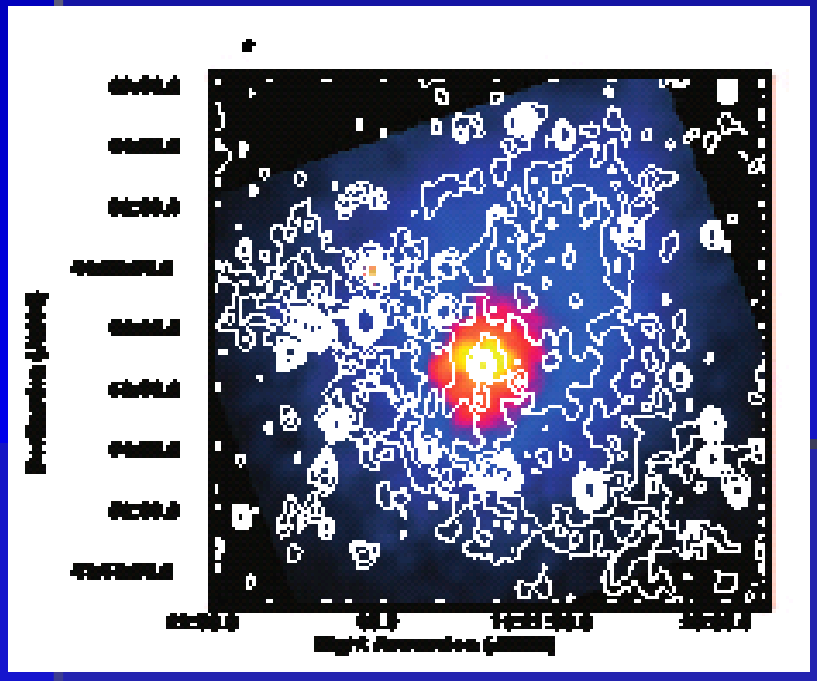

Rosat X-ray image (colors)
Radio image (contours)
Feretti et al. 1997

Lline-of-sight velocity distribution of member galaxies

A2319A
15727±139km/s

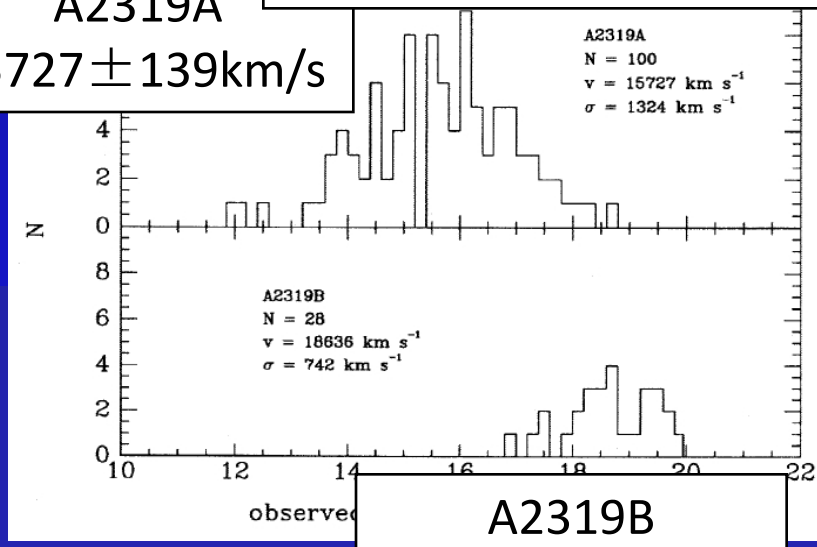

A2319B
18636±151km/s

Oegerle et al.1995

Line-of-sight Velocities of the ICM

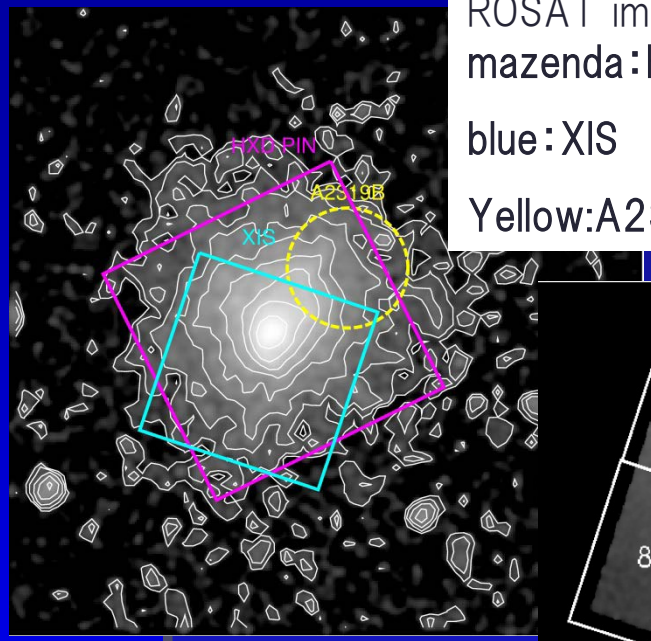

ROSAT image
mazenda：HXD PIN、
blue：XIS
Yellow:A2319B

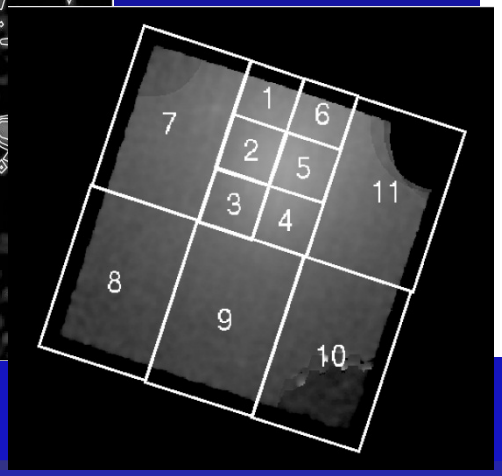

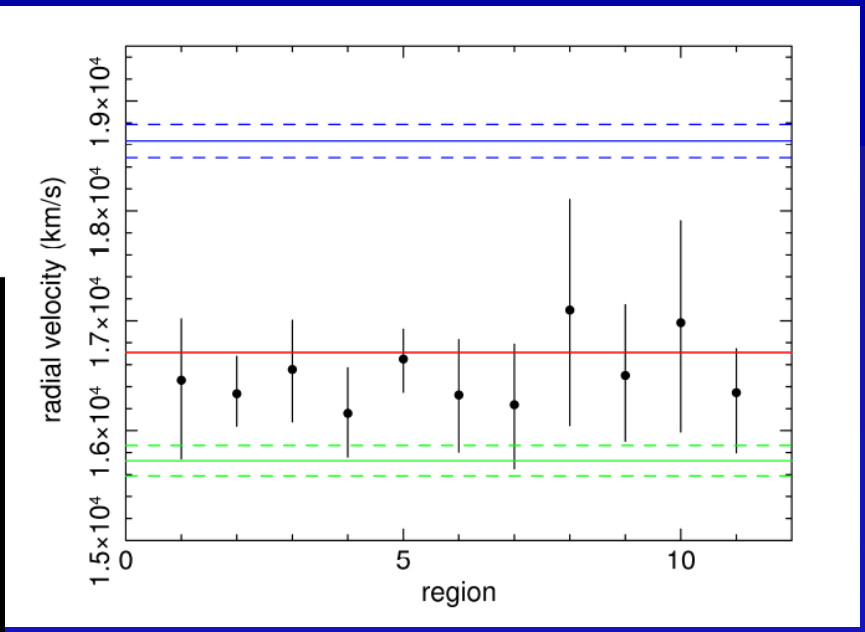

- It is clear that the observed velocities are different from that of A2319B subgroup.
- No significant velocity difference is detected within the observed region.
- $\Delta v < 940^{+1083}_{-1131}$ km/s. (cf. $c_s \sim 1700$ km/s)

Line-of-sight velocity

Blue: A2319B subgroup
Green: A2319A subgroup
Red: A2319

Wide band spectrum

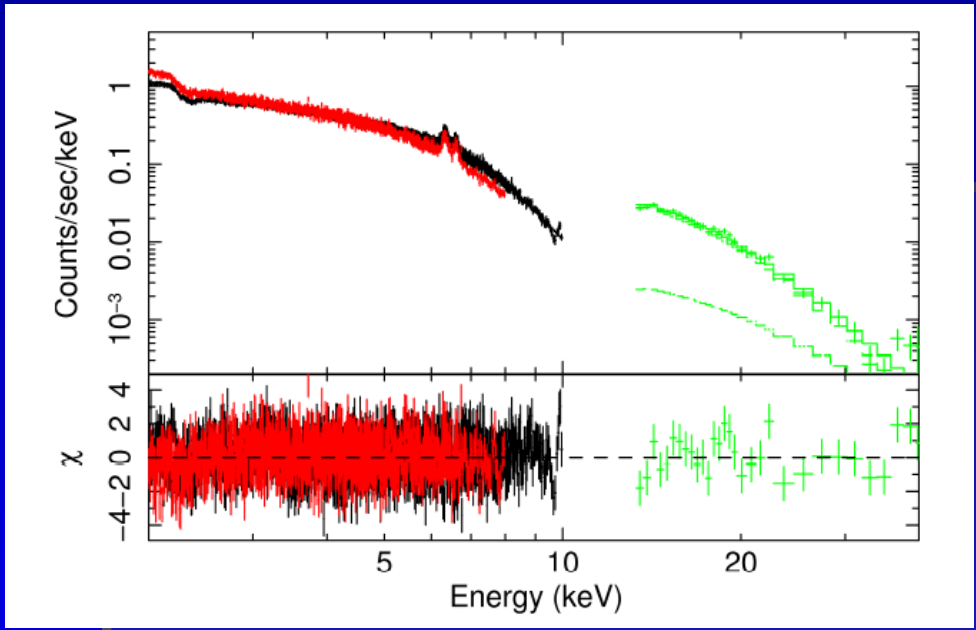

Wide band spectrum fitted with APEC+Powerlaw model

Black: XIS FI
Red: XIS BI
Green: PIN

Flux of a power-law component in 10-40 keV and its upper limits

model	flux (erg s^{-1} cm^{-2})	upper limit (erg s^{-1} cm^{-2})
$1kT + PL(1.92)$	$1.1^{+0.8+1.3}_{-0.8-1.1} \times 10^{-11}$	$< 2.6 \times 10^{-11}$
$1kT + PL(2.4)$	$1.5^{+1.2+1.9}_{-1.2-2.1} \times 10^{-11}$	$< 3.8 \times 10^{-11}$
$2kT + PL(1.92)$	$0.0^{+3.7+2.2}_{-0.0-0.0} \times 10^{-11}$	$< 4.3 \times 10^{-11}$
$2kT + PL(2.4)$	$0.0^{+2.2+3.9}_{-0.0-0.0} \times 10^{-11}$	$< 4.5 \times 10^{-11}$

The lower limit of the magnetic field strength

model	$B(\mu G)$
$1kT + PL(1.92)$	> 0.19
$1kT + PL(2.4)$	> 0.27
$2kT + PL(1.92)$	> 0.14
$2kT + PL(2.4)$	> 0.25

Energy Budget of the Intracluster space

Thermal Energy

- ROSAT image → $n_e(r)$
- kT=10keV

$$U_{\rm th} = 0.4 \times 10^2 \ {\rm eV/cm^3}$$

Abell 2319

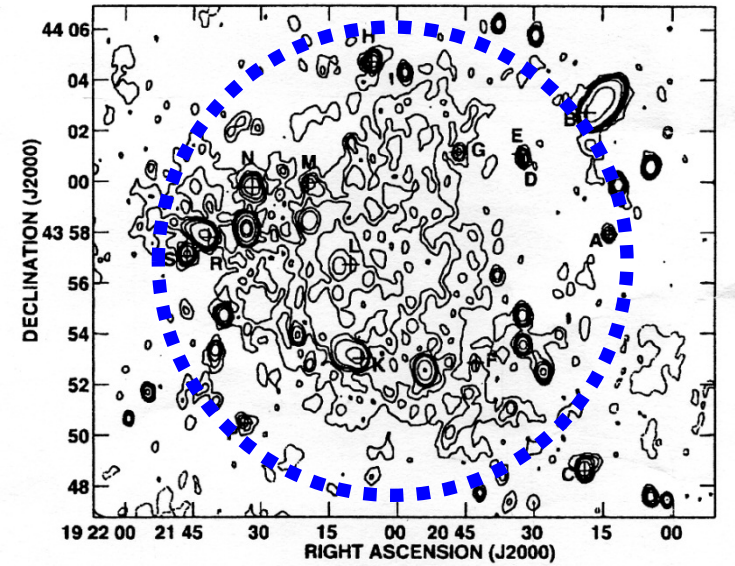

Feretti et al.1997

Magnetic Energy

- **Suzaku Results (>0.2μG)**

$$U_B > 0.1 \times 10^{-2} \ {\rm eV/cm^3}$$

$U_B/U_{th} > 3 \times 10^{-5}$

CR electrons ($5.7 \times 10^3 < \gamma < 1.1 \times 10^4$)

- Suzaku results (upper limit of hard X-ray)

$$U_e < 0.2 \times 10^{-1} \ {\rm eV/cm^3}$$

$U_e/U_{th} < 5 \times 10^{-4}$

ZwCl 0823.2+0425 Field

Optical image and the mass contours
With XIS FOV.

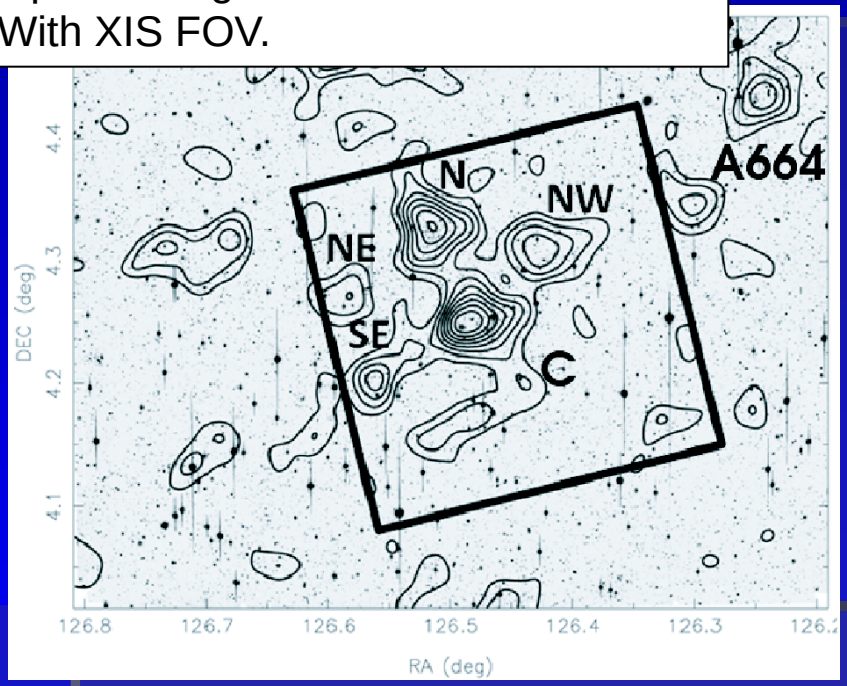

ROSAT image

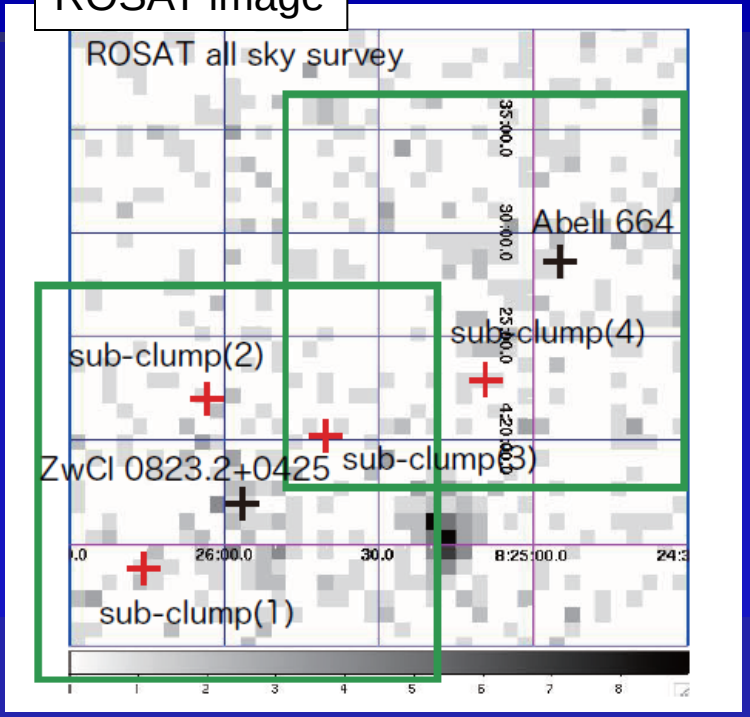

- Several dark halos were found by a weak lensing survey (Okabe et al. 2010).
- No deep X-ray image.
- L_X???, kT???, Metal Abundance????

Results(1)

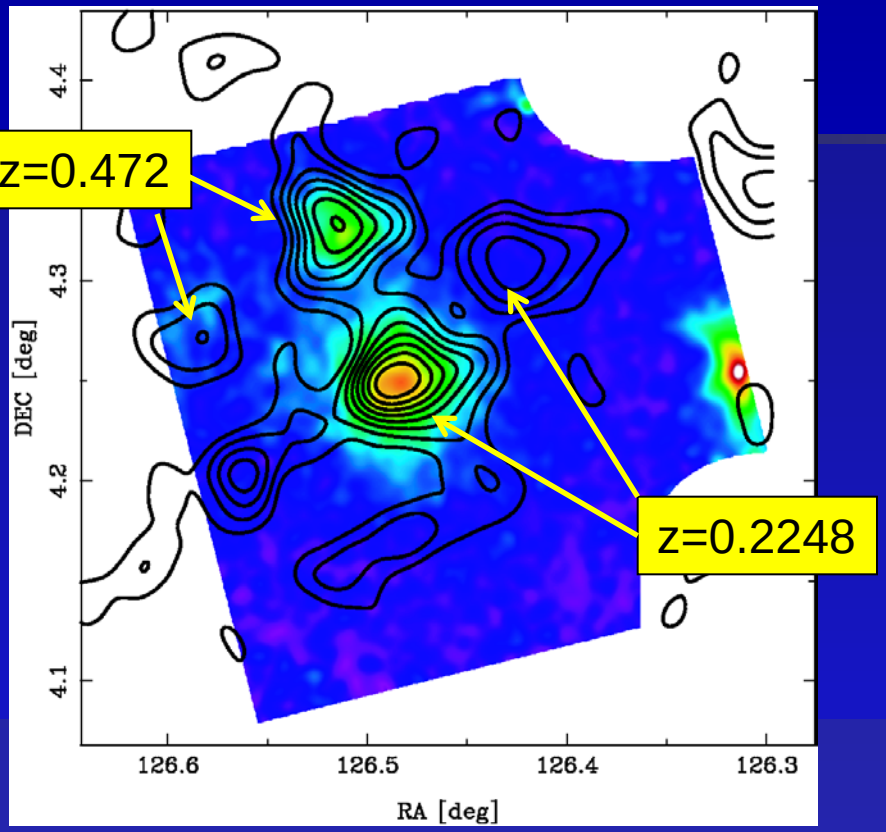

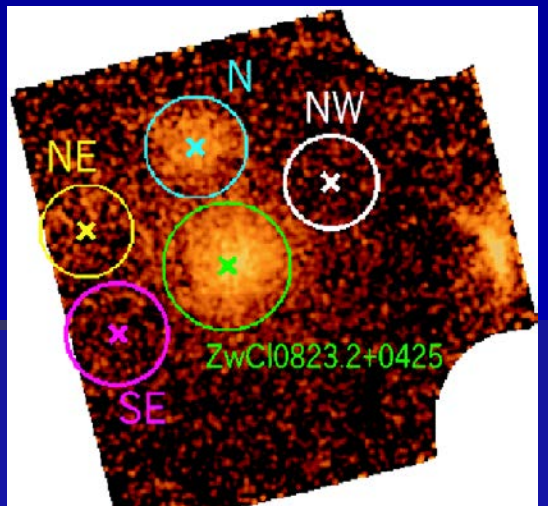

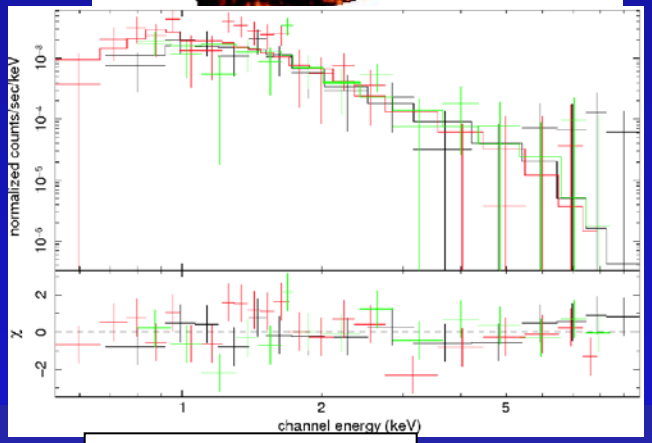

NW spectrum

- Significant excess X-ray signals except for SE
- kT determination except for SE
- Metal Abundance determination for C and N

Results(2)

M-T relation

Best fit (solid line)

$$M_{500}E(z) = 2.63^{+0.81}_{-0.63}\left(\frac{k_{\rm B}T}{5\ {\rm keV}}\right)^{2.38^{+0.78}_{-0.95}} \times 10^{14}h^{-1}M_{\odot}, \quad (8)$$

Assuming $M \propto T^{3/2}$ (solid line)

$$M_{500}E(z) = 2.47^{+0.69}_{-0.57}\left(\frac{k_{\rm B}T}{5\ {\rm keV}}\right)^{3/2} \times 10^{14}h^{-1}M_{\odot}, \quad (9)$$

Normalization is consistent with results of X-ray selected sample (Okabe et al. 2010)

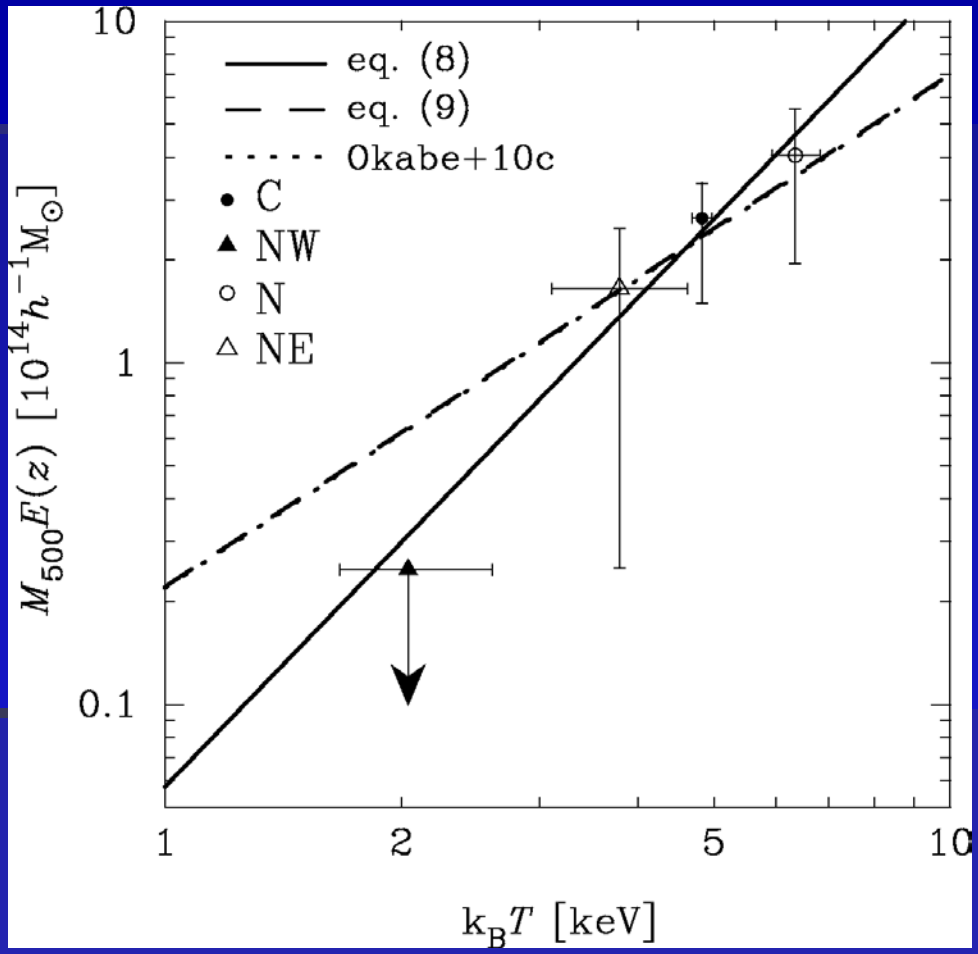

Sunyaev-Zel'dovich 効果

逆コンプトン散乱

CMB光子
(2.7K
black body)

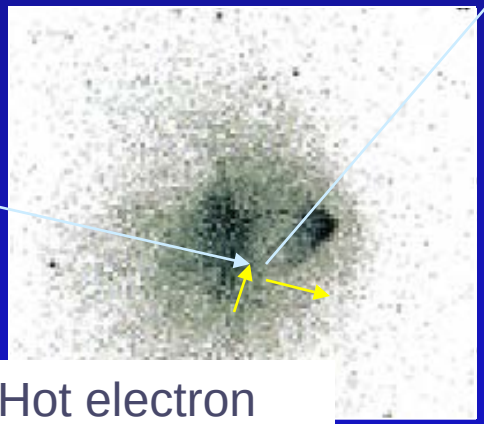

Hot electron
($10^{7\text{-}8}$K)

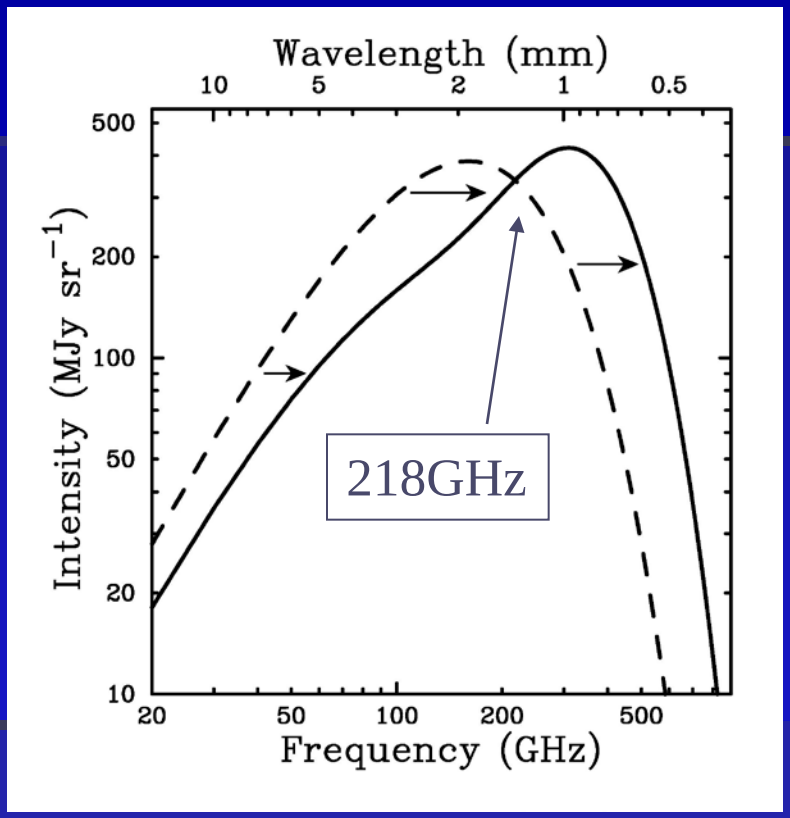

銀河団(など)の高温ガスによる逆コンプトン散乱で
Cosmic Microwave Background (CMB) のスペクトルが変形。

- ミリ波帯(R-J側)ではdecrement
- サブミリ波帯(Wein側)ではincrement

(Thermal) SZ vs X-ray

$I_X \propto \int n_e^2 T_e^{1/2} dl$

$I_{SZ} \propto \int n_e T_e dl$

X線は密度構造に、SZは温度構造によりsensitive。

$I_X \propto (1+z)^{-4}$

$I_{SZ} \propto (1+z)^0$ （$U_{CMB} \propto (1+z)^4$なため）

high z object にはSZが有利

Imaging Simulation for ALMA

X-ray image and kT made from hydro sim. (Takizawa 2005)

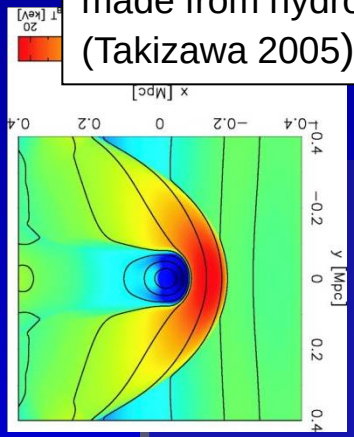

SZ observation with ALMA
（Yamada et al. 2012）

more sensitive to high kT component such as shocks

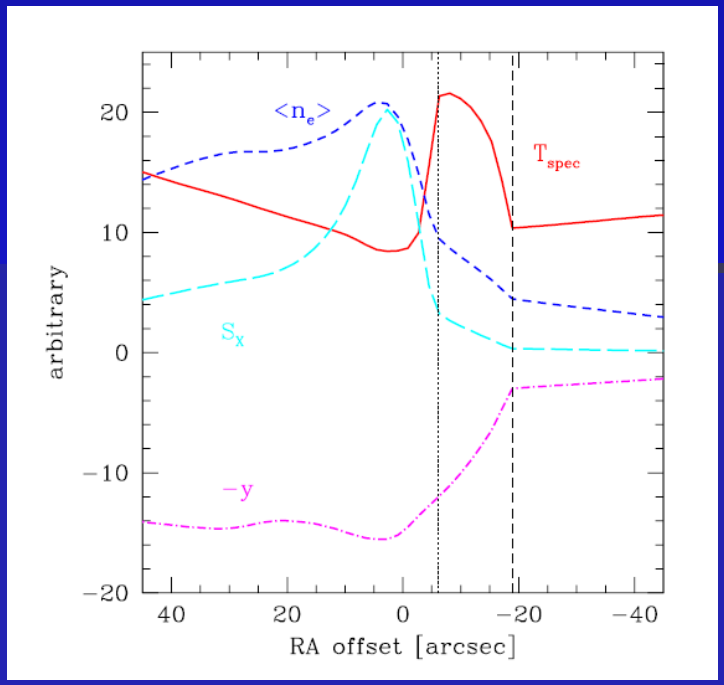

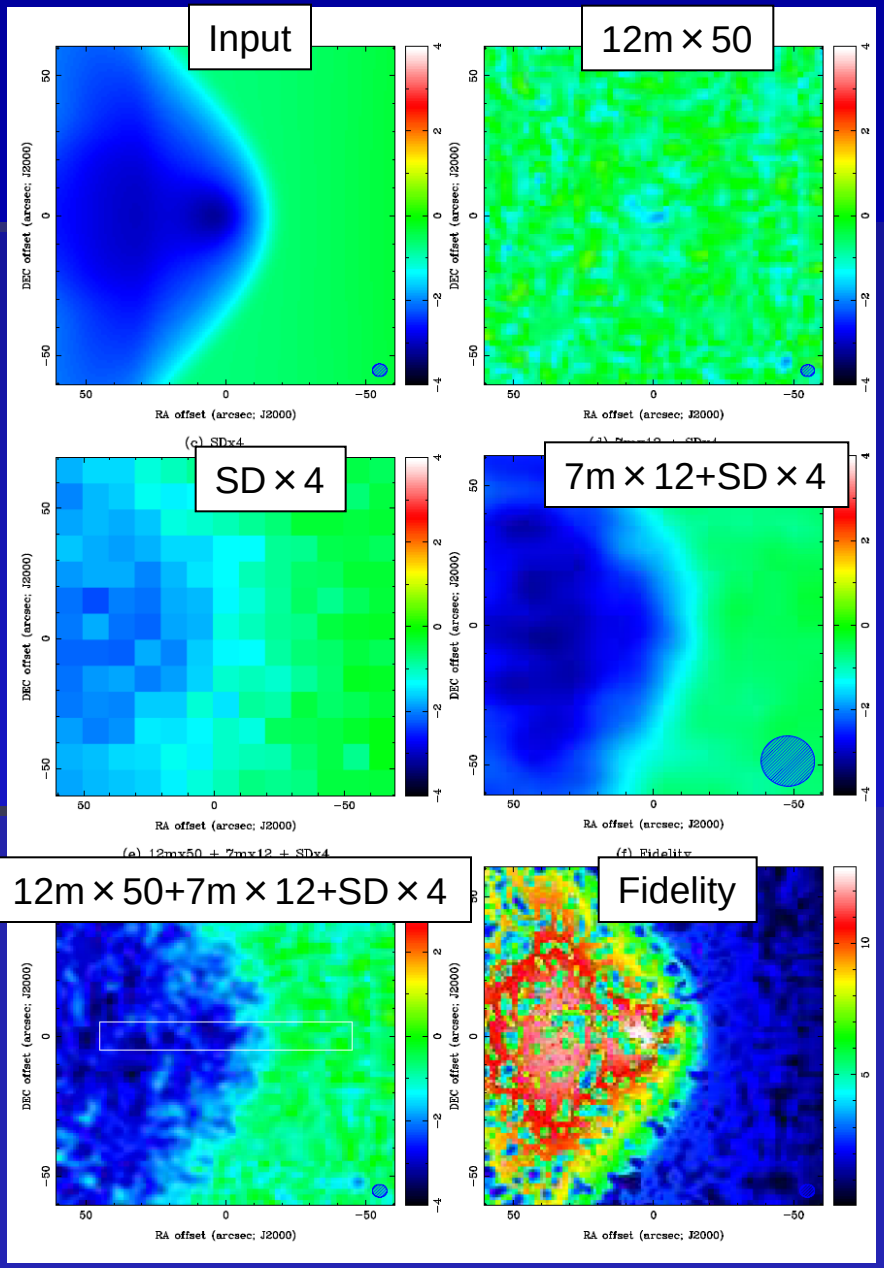

Summary

- A2319
  - Line-of-sight velocities of the ICM
  - Constraint of the energy density of the magnetic field and CR electrons through the non-thermal hard X-ray upper limit
- ZwCl0823.2+0425 Field
  - X-ray follow-up observation of weak-lensing-detected halos
  - Self-similar M-T relation consistent with X-ray selected sample
- Imaging simulations of SZE for ALMA

  ALMA + ACA will resolve the ICM shock structures in its most compact configuration at 90 GHz.